

## A controllable viewing angle LCD with an optically isotropic liquid crystal

This article has been downloaded from IOPscience. Please scroll down to see the full text article.

2010 J. Phys. D: Appl. Phys. 43 145502

(<http://iopscience.iop.org/0022-3727/43/14/145502>)

[The Table of Contents](#) and [more related content](#) is available

Download details:

IP Address: 132.170.56.214

The article was downloaded on 25/03/2010 at 13:55

Please note that [terms and conditions apply](#).

# A controllable viewing angle LCD with an optically isotropic liquid crystal

Min Su Kim<sup>1</sup>, Young Jin Lim<sup>1</sup>, Sukin Yoon<sup>1</sup>, Shin-Woong Kang<sup>1</sup>,  
Seung Hee Lee<sup>1</sup>, Miyoung Kim<sup>2</sup> and Shin-Tson Wu<sup>3</sup>

<sup>1</sup> Department of BIN Fusion Technology and Department of Polymer-Nano Science and Technology, Chonbuk National University, Jeonju, Jeonbuk 561-756, Korea

<sup>2</sup> Korea Electronics Technology Institute, Jeonju, Jeonbuk 561-844, Korea

<sup>3</sup> College of Optics and Photonics, University of Central Florida, Orlando, FL 32816, USA

E-mail: [lsh1@chonbuk.ac.kr](mailto:lsh1@chonbuk.ac.kr) and [swu@creol.ucf.edu](mailto:swu@creol.ucf.edu)

Received 5 December 2009, in final form 25 February 2010

Published 23 March 2010

Online at [stacks.iop.org/JPhysD/43/145502](http://stacks.iop.org/JPhysD/43/145502)

## Abstract

An optically isotropic liquid crystal (LC) such as a blue phase LC or an optically isotropic nano-structured LC exhibits a very wide viewing angle because the induced birefringence is along the in-plane electric field. Utilizing such a material, we propose a liquid crystal display (LCD) whose viewing angle can be switched from wide view to narrow view using only one panel. In the device, each pixel is divided into two parts: a major pixel and a sub-pixel. The main pixels display the images while the sub-pixels control the viewing angle. In the main pixels, birefringence is induced by horizontal electric fields through inter-digital electrodes leading to a wide viewing angle, while in the sub-pixels, birefringence is induced by the vertical electric field so that phase retardation occurs only at oblique angles. As a result, the dark state (or contrast ratio) of the entire pixel can be controlled by the voltage of the sub-pixels. Such a switchable viewing angle LCD is attractive for protecting personal privacy.

(Some figures in this article are in colour only in the electronic version)

## 1. Introduction

The basic light modulation mechanism of most liquid crystal display (LCD) devices is based on electric field induced molecular reorientation which in turn gives rise to phase retardation. The effective birefringence of the LC panel is dependent on the viewing angle. As the LCD size gets larger the viewing angle issue becomes more serious. Several wide view technologies, such as in-plane switching (IPS) [1], fringe-field switching (FFS) [2] and multi-domain vertical alignment (MVA) [3], have been developed. For display uses, two different situations are often encountered: group viewing and privacy viewing. The former demands a wide viewing angle device, but the latter prefers a narrow view in order to protect personal or confidential information. To realize controllable viewing angle, two different approaches have been developed: one with an addition of a viewing angle control panel [4–7] and the other with a pixel division into a main pixel and a sub-pixel for displaying images and controlling the viewing angle, respectively [8–11].

Recently, polymer-stabilized blue phase (BP) LC has been emerging for LCD applications because it does not require any alignment layer [12, 13] and its response time is in hundreds of microseconds [14–18]. From a macroscopic viewpoint, BP LC is optically isotropic in the voltage-off state. While in a voltage-on state, the Kerr effect induced birefringence is along the electric field direction [12, 13]. Therefore, a BPLCD addressed by a transversal electric field exhibits a fairly wide and symmetric viewing angle.

In this paper, we propose a switchable viewing angle LCD using an optically isotropic LC for the first time. In the device, each pixel is divided into two parts: a main pixel and a sub-pixel. The main pixel displays the image contents, while the sub-pixel controls the viewing angle. In the main pixel, the birefringence is induced by transversal electric fields so that the displayed images are insensitive to viewing angle because the LC reorientations are in the same plane. However, in the sub-pixels the birefringence is induced by longitudinal electric fields, i.e. the optic axis of the LC is perpendicular to the substrates. As a result, the phase retardation of the

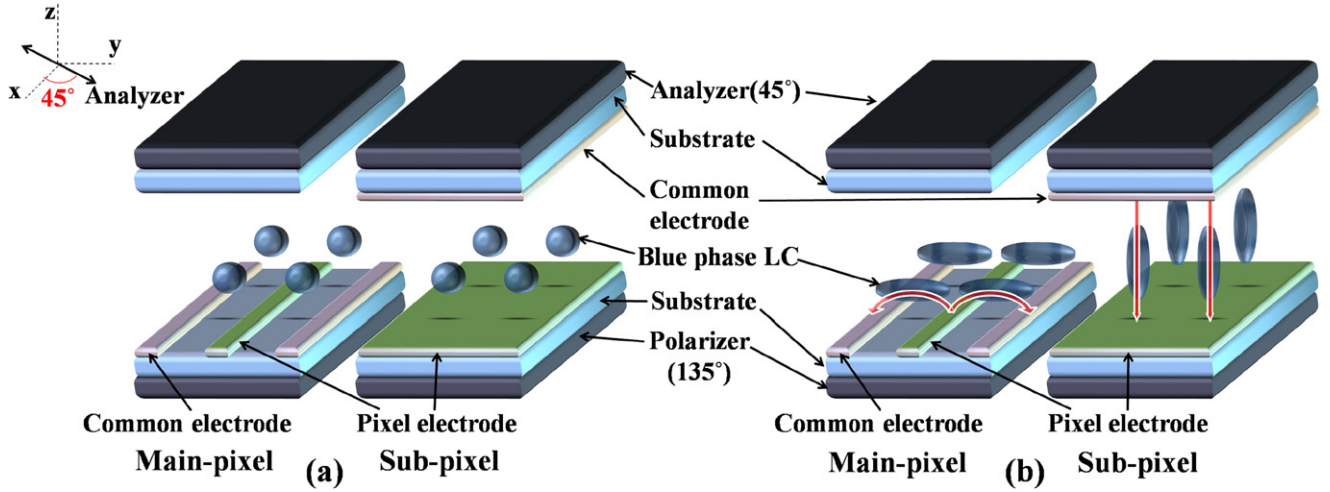


**Figure 1.** Device configuration of the viewing angle switchable LCD with an optically isotropic LC: (a) voltage-off state and (b) voltage-on state.

LC causes light leakage in the oblique viewing directions and the leakage level can be controlled by the applied voltage. Depending on the applied voltage, the light leakage in viewing directions can be controlled while keeping zero retardation in the normal direction when the main image is displayed. With this operating principle, the viewing angle of the LCD is switchable.

## 2. Cell structure and switching principle

In figure 1, the proposed device consists of main pixels and sub-pixels filled with a BP LC and the cell is sandwiched between crossed polarizers. In the main pixels, the pixel and the common electrodes are interdigitated on the inner surface of the bottom substrate, whereas in the sub-pixels the pixel and the common electrodes are on the bottom and top substrates. When a voltage is applied between two electrodes, in-plane and vertical electric fields are generated in the main pixels and sub-pixels, respectively. Without a bias voltage, the BP LC is optically isotropic as represented by the spheres in figure 1(a). With a bias voltage, the birefringence as represented by the ellipse is induced by the Kerr effect as shown in figure 1(b) and its optic axes are parallel and perpendicular to the substrate in the main pixels and the sub-pixels, respectively.

When an external electric field is applied to a uniaxial medium ( $\Delta n = n_e - n_o$ ) such as a nematic liquid crystal, the dielectric tensor has different magnitudes parallel and perpendicular to the director. Thus an applied electric field couples to the directors which means an optic axis of birefringence can be determined by the electric field direction. It can be calculated by Landau–de Gennes theory. For a BP LC, the amplitude of the induced birefringence ( $\Delta n_i$ ) which is formed in a local region of the polymer network mesh along the field direction is determined by the following Kerr equation [19–21]:

$$\Delta n_i = \lambda K E^2, \quad (1)$$

where  $\lambda$  is the wavelength,  $K$  the Kerr constant of the BP LC and  $E$  the electric field intensity.

To calculate the device performance, we employed the three-dimensional commercial simulation software ‘Techwiz LCD’ (Sanayi System, Korea). We have developed a numerical solver to characterize the electro-optical properties of a polymer-stabilized BP LC cell. Our model is based on calculating the induced birefringence by the Kerr effect of BP LC. Our approach is composed of three steps: (1) calculating the  $E$ -field distribution in the media of BP LC by solving the Laplace equation; (2) calculating the induced birefringence and its optic axis from the calculated  $E$  field; and (3) calculating the transmittance by the  $2 \times 2$  extended Jones matrix technique. In our model, we assume that the induced birefringence cannot exceed the birefringence ( $\Delta n_h$ ) of the LC composite since polymer-stabilized BP LC is a combination of nano-structured host LC with nematic-like short-range ordering and polymer network. Similar approach has been reported by Ge *et al* [22]. Therefore, we set a constraint as follows:

$$\Delta n_i \leq \Delta n_h, \quad \text{where } |\vec{E}| > \sqrt{\frac{\Delta n_h}{\lambda K}}. \quad (2)$$

Moreover, we also considered BP LC as an electrically isotropic material with an effective dielectric constant ( $\epsilon_{BP} = \epsilon_{\perp} + \frac{1}{3} \Delta \epsilon$ ) in the  $E$ -field calculation because of its macroscopic structural symmetry.

In the device, the normalized light transmittance ( $T$ ) of the device associated with the phase retardation can be characterized as follows:

$$T = \sin^2 2\psi \times \sin^2 \{ \pi d \Delta n_i (V) / \lambda \}, \quad (3)$$

where  $\psi$  is an angle between one of the transmission axes of the crossed polarizers and the optic axis of BP LC director,  $d$  is the LC layer thickness with induced birefringence. Without bias voltage,  $\Delta n_i$  is equal to zero so that the device appears to be dark not only in the normal direction but also in the oblique viewing directions. With bias voltage and conditions of  $\psi = 45^\circ$  and  $d \Delta n_i = \lambda/2$ , a maximum bright state is achieved in the main-pixel region.

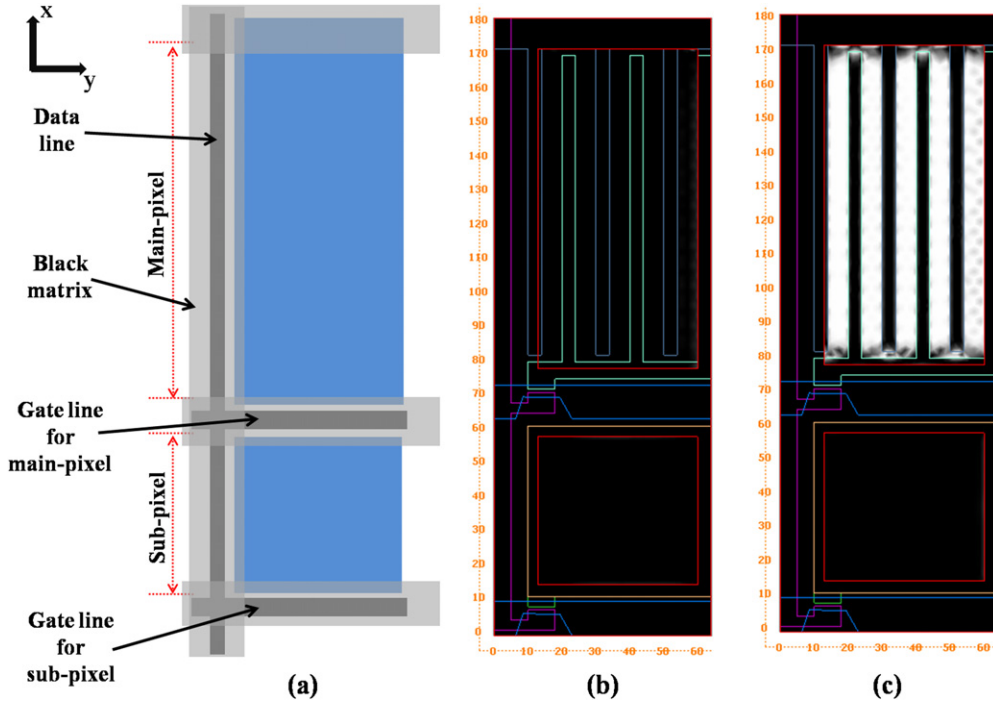


**Figure 2.** (a) Schematic configuration of the pixel structure, (b) dark state and (c) bright state with  $19 \text{ V } \mu\text{m}^{-1}$  with black matrix in the pixel for both narrow and wide viewing angle modes.

To realize a wide viewing angle, only the main pixels are operated while the sub-pixels are turned off. The device exhibits a good dark state in all viewing directions because the employed BP LC is optically isotropic under crossed polarizers, and good uniformity in the bright state because the induced retardation is along the in-plane electric fields. As a result, the viewing angle is wide. To realize a narrow viewing angle, a voltage is applied to the sub-pixels while the image is displayed by the main pixels. Here, the induced optic axis of the LC is perpendicular to the substrates ( $\psi = 0^\circ$ ) so that the sub-pixels appear black in the normal direction; however, light leakage occurs in the oblique viewing directions except for those coincident with the polarizer's transmission axis. Using the described light leakage, the main displayed images are obscured in the oblique viewing directions.

### 3. Results and discussion

To demonstrate the controllable viewing angle characteristics of the proposed device, we performed a simulation using the TechWiz software. In the main pixels, the electrode width is  $w = 4 \mu\text{m}$ , electrode gap  $l = 6 \mu\text{m}$ , the LC layer thickness  $d = 10 \mu\text{m}$  and the Kerr constant  $K = 1 \text{ nm V}^{-2}$ .

Figure 2(a) shows the schematic pixel structure of the viewing angle switchable device in which the pixel is comprised of a main pixel and a sub-pixel, and the gate and data lines provide electrical signals to the pixel electrode, with an optimized design of black matrix to block the light leakage in the area between the signal and the pixel electrodes [9]. A complete dark state for the sub-pixel and the main pixel is achieved in the normal direction as shown in figure 2(b). With a bias voltage ( $19 \text{ V } \mu\text{m}^{-1}$ ) for fully white state in both pixels,

the main pixel shows transmittance whereas the sub-pixel shows no transmittance, as figure 2(c) shows. In order to achieve a fully white state, an electric field of about  $19 \text{ V } \mu\text{m}^{-1}$  is applied to the main pixel while  $14 \text{ V } \mu\text{m}^{-1}$  is applied to the sub-pixel. In the sub-pixel, the electric field is in the vertical direction, and so is the induced birefringence. As a result, the transmittance does not occur in the sub-pixel in the normal viewing direction. However, as depicted in figure 3 a light leakage occurs at oblique angles mainly in the diagonal directions except those along the polarizer axis. This is because the incident polarized light experiences a phase retardation by the induced birefringence with its optic axis perpendicular to the substrate. The light leakage occurs mainly in the vertical and horizontal directions of the panel (these are the bisectors of the transmissive axes of the crossed polarizers, of which the azimuthal angles are  $\varphi = 0^\circ, 90^\circ, 180^\circ$  and  $270^\circ$ , respectively). Figure 3 clearly shows that as the viewing direction increases over  $10^\circ$  of the polar angle in both horizontal and vertical directions, the light leakage starts to occur and reaches a maximum between  $40^\circ$  and  $60^\circ$  of the polar angle depending on the applied voltage. From figure 3, the largest light leakage takes place at  $14 \text{ V } \mu\text{m}^{-1}$  at  $45^\circ$  polar angle. As the applied field increases to  $15 \text{ V } \mu\text{m}^{-1}$ , the maximum transmittance occurs at  $40^\circ$ . So, for a proper viewing angle control the electric field of  $14 \text{ V } \mu\text{m}^{-1}$  can be chosen.

The operation principle and the associated light leakage of the proposed device configuration can be described on the Poincaré sphere as follows. Poincaré sphere representation is an elegant geometrical means for analysing the propagation of polarized light through birefringent and optically active media [23]. Figure 4 shows the polarization path of the light passing through the cell on the three-dimensional Poincaré

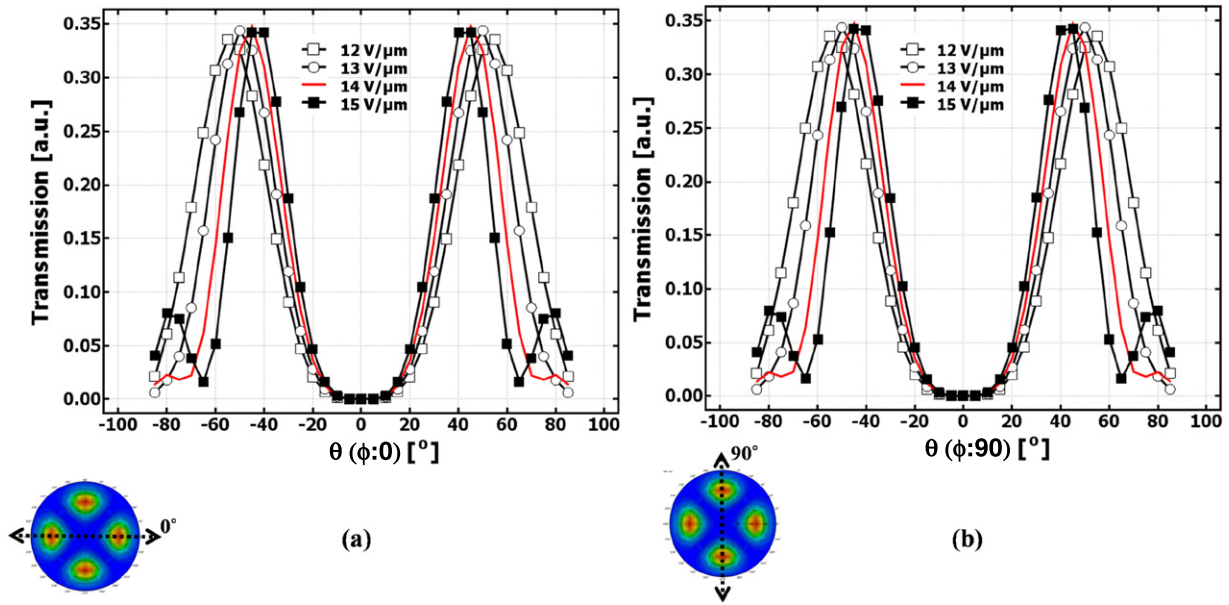


**Figure 3.** Simulated viewing angle dependent transmittance according to the polar angles by horizontal direction: (a) azimuthal 0–180° and (b) azimuthal 90–270° in the sub-pixel.

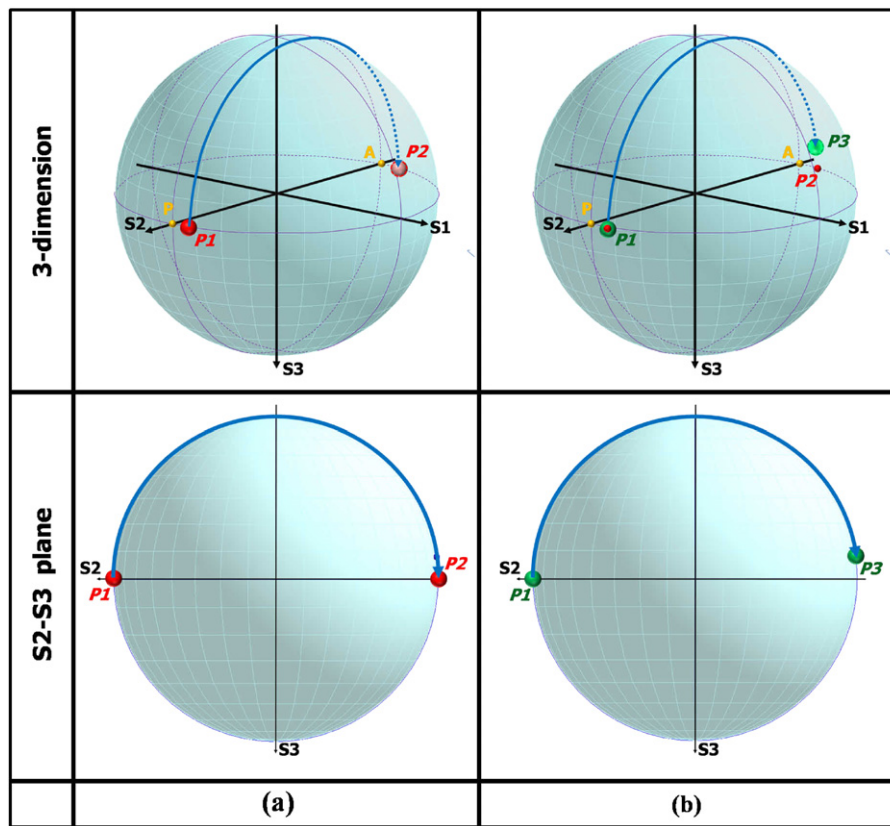


**Figure 4.** Poincaré sphere representation of the polarization path of (a)  $\lambda/2$  retardation value in 45° oblique direction and in (b) the sub-pixel in 45° oblique viewing angle at 0° azimuthal angle.

sphere which indicates three coordinates ( $S_1$ ,  $S_2$ ,  $S_3$ ) on the surface of a unit sphere and  $S_2$ – $S_3$  plane. The arrow lines from  $P_1$  to  $P_2$  and  $P_1$  to  $P_3$  in figure 4 represent the polarization state of the light and  $P$  (0, 1, 0) and  $A$  (0, -1, 0) indicate the polarization positions of the polarizer ( $\varphi = 135^\circ$ ) and the analyzer ( $\varphi = 45^\circ$ ), respectively. For the reference of

the maximum bright state in the sub-pixel of the device, an LC layer with  $\lambda/2$  phase retardation at  $\lambda = 550$  nm and 45° oblique viewing angle under crossed polarizers is assumed, as shown in figure 4(a). In the normal viewing direction of a sub-pixel, the polarization of the light passing through the LC layer with its induced birefringence perpendicular to the substrates

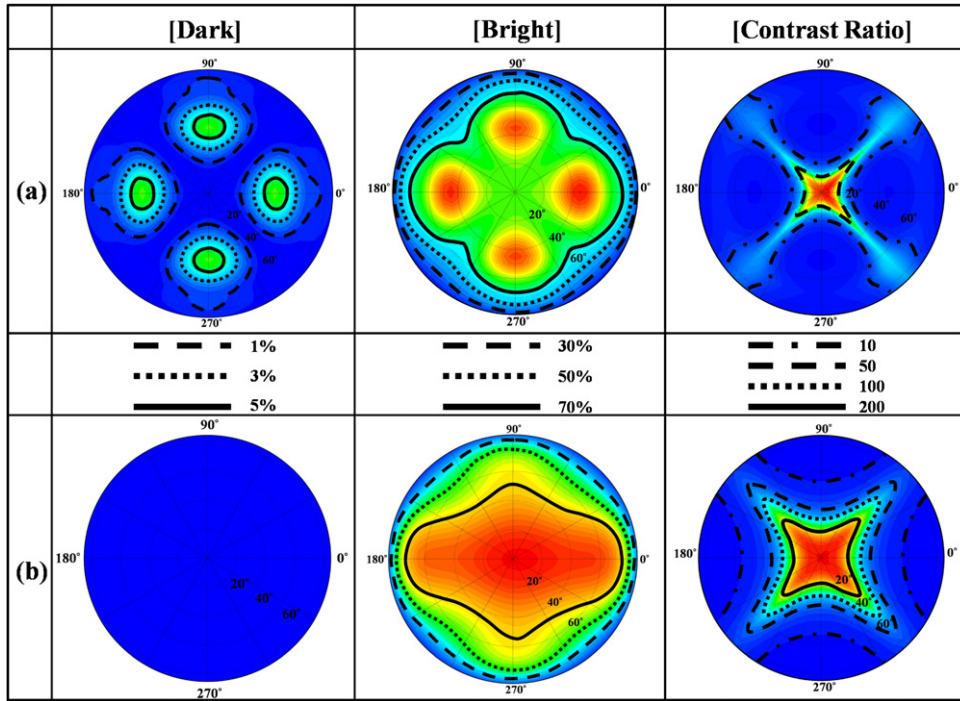


**Figure 5.** Iso-transmittance curves in the dark and bright states and iso-contrast ratio curves: (a) narrow viewing angle mode and (b) wide viewing angle mode.

stays at position  $P$ , which implies the linear polarization on the Poincaré sphere even if the voltage is applied.

In the case of the  $45^\circ$  oblique viewing angle, the starting position of the light propagating through the polarizer is set at position  $P1$ . The position  $P1$  moves to an opposite position  $P2$  when the light passes through the LC layer which behaves like a half-wave plate. That is to say, the direction of linear polarization is changed to a crossed direction which is the same as the analyzer's transmission axis. Under off-axis oblique view, the two orthogonally crossed polarizers are no longer perpendicular as visualized, so that the exact opposite side (by holding the point  $(0, 0, 0)$  as a criterion position) of  $P1$  is no longer a maximum bright state. In oblique viewing, the angle between crossed polarizers is determined as  $2 \tan^{-1}(\cos \theta)$  [24], where  $\theta$  is the polar angle. Thus the actual angle of the crossed polarizers is calculated to be  $\sim 70.53^\circ$ , which means the position of the maximum bright state should be  $P2$ . This is an ideal condition in the case of  $45^\circ$  oblique viewing angle which generates maximum light leakage as expected from equation (3). However, as shown in figure 4(b) in a real device position  $P$  will be slightly deviated to  $P1$  where it is observed in an oblique polar angle of  $45^\circ$  at the bisector position of the crossed polarizers, and then position  $P1$  will move to  $P3$  after propagating through the LC layer at  $14 \text{ V } \mu\text{m}^{-1}$ . As mentioned above, the maximum transmittance would be achieved if  $P1$  moves to  $P2$  at  $45^\circ$  oblique viewing angle; instead, it moves from  $P1$  to  $P3$ . Nevertheless, it achieves almost maximum transmittance even though  $P3$  is not exactly the point for maximum transmittance. The calculated retardation value is  $274 \text{ nm}$ , very close to  $275 \text{ nm}$  at  $\varphi = 0^\circ$ , and  $\theta = 45^\circ$ .

Finally, the iso-transmittance curves in the dark and bright states and the iso-contrast ratio curves from the perspective

of switching performance are calculated for both narrow- and wide-view modes, as shown in figures 5(a) and (b), respectively. The 30%, 50% and 70% iso-transmittance curves correspond to the relative values with respect to the maximum transmittance in the bright state of the wide-view mode and iso-transmittance curves of 5%, 3% and 1% correspond to the relative value with respect to the incident light in the dark state of the whole pixel. In both cases, the maximum light leakage for wide- and narrow-view modes is 1.7% and 34.8%, respectively. In the bright state, the area in which the transmittance is in excess of 30% with respect to the transmittance in the normal direction exists over  $\sim 80^\circ$  polar angle in all azimuthal directions of both wide- and narrow-view modes. On the other hand, in the dark state light leakage is significantly suppressed in the wide-view mode but the light leakage in the narrow-view mode occurs intensively at the upper, the lower, the left and the right sides, particularly along about  $30^\circ$ – $60^\circ$  of the polar angle, as figure 5(a) shows. As a result, for the wide-view mode the contrast ratio ( $>10 : 1$ ) exists up to  $\sim 50^\circ$  of the polar angle in all azimuthal directions (figure 5(b)), whereas for the narrow-view mode the 10 : 1 iso-contrast ratio contour exists just along  $20^\circ$  of the polar angle in the horizontal and the vertical directions (figure 5(a)).

To confirm the performance of the proposed device, the quality of the displayed images is calculated as shown in figure 6. In the wide-view mode (figure 6(a)), the original image is well perceived in all viewing angles because the device is represented only by the main pixels in which the birefringence is induced along the in-plane electric fields. In contrast, in the narrow-view mode, the original image is not perceived well in the four polar directions as shown in figure 6(b). These simulated results demonstrate the

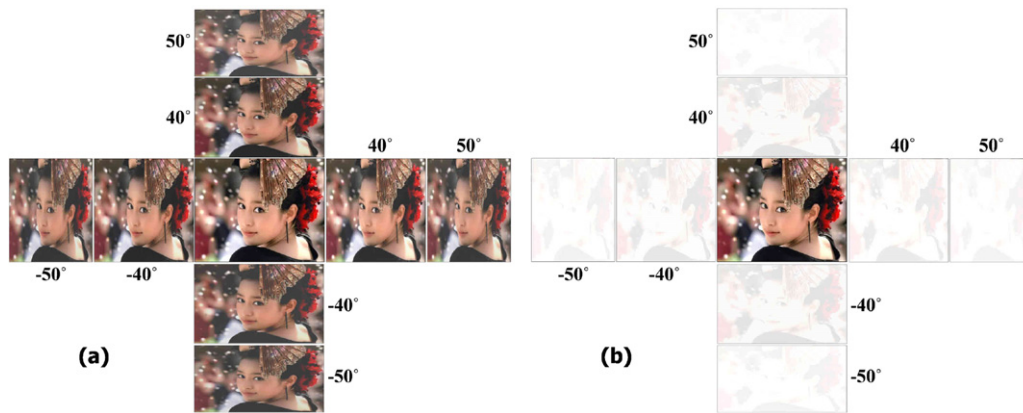


**Figure 6.** Dependence of the displayed images according to the viewing angle: (a) wide viewing angle mode and (b) narrow viewing angle mode.

outstanding effect on the viewing angle switching of the proposed device.

#### 4. Summary

A controllable viewing angle liquid crystal device based on the Kerr effect is proposed for the first time. The pixel consists of two parts: a main pixel and a sub-pixel. In the main pixel, the in-plane electric field is used for displaying images with a wide viewing angle while in the sub-pixel the vertical field is used for realizing a narrow viewing angle. Unlike the conventional viewing angle switchable device which controls only in the horizontal direction, the proposed device can control the viewing angles in both horizontal and vertical directions.

#### Acknowledgments

This work was supported by the WCU programme through MEST (R31-2008-000-200029-0) and by the Selection of Research-oriented Professor Programme of Chonbuk National University in 2009.

#### References

- [1] Oh-e M and Kondo K 1995 *Appl. Phys. Lett.* **67** 3895
- [2] Lee S H, Lee S L and Kim H Y 1998 *Appl. Phys. Lett.* **73** 2881
- [3] Lee S H, Kim S M and Wu S T 2009 *J. Soc. Inform. Disp.* **17** 551
- [4] Jin H S, Chang H S, Park J K, Yu S K, Lee D S and Chung I J 2006 *Soc. Inform. Disp. Symp. Digest* **37** 729
- [5] Hiyama Y K, Ogawa R, Ishinabe T and Uchida T 2006 *Proc. Int. Display Workshop (Society for Information Display, Otsu, Japan)* p 217
- [6] Adachi M 2008 *Japan. J. Appl. Phys.* **47** 7920
- [7] Jeong E, Lim Y J, Rhee J M, Lee S H, Lee G D, Park K H and Choi H C 2007 *Appl. Phys. Lett.* **90** 051116
- [8] Lim Y J, Jeong E, Kim Y S, Rhee J M, Lee G D and Lee S H 2007 *Soc. Inform. Disp. Symp. Digest* **38** 756
- [9] Lim Y J, Jeong E, Chin M H, Ji S, Lee G D and Lee S H 2008 *J. Phys. D: Appl. Phys.* **41** 085110
- [10] Jeong E, Lim Y J, Chin M H, Kim J H, Lee S H, Ji S H, Lee G D, Park K H, Choi H C and Ahn B C 2008 *Appl. Phys. Lett.* **92** 261102
- [11] Lim Y J, Jeong E, Kim Y S, Jeong Y H, Jang W G and Lee S H 2008 *Mol. Cryst. Liq. Cryst.* **495** 186
- [12] Hisakado Y, Kikuchi H, Nagamura T and Kajiyama T 2005 *Adv. Mater.* **17** 96
- [13] Sato M and Yoshizawa A 2007 *Adv. Mater.* **19** 4145
- [14] Kikuchi H, Yokota M, Hisakado Y, Yang H, Kajiyama T 2002 *Nature Mater.* **1** 64
- [15] Haseba Y, Kikuchi H, Nagamura T and Kajiyama T 2005 *Adv. Mater.* **17** 2311
- [16] Haseba Y, Kikuchi H 2006 *J. Soc. Inform. Disp.* **14** 551
- [17] Noma T, Ojima M, Asagi H, Kawahira Y, Fujii A, Ozaki M and Kikuchi H 2008 *e-J. Surf. Sci. Nanotechnol.* **6** 17
- [18] Choi S W, Yamamoto S, Haseba Y, Higuchi H and Kikuchi H 2008 *Appl. Phys. Lett.* **92** 043119
- [19] Kerr J 1875 *Philos. Mag.* **50** 337
- [20] Rao L, Ge Z and Wu S-T 2010 *Opt. Express* **18** 3143
- [21] Kikuchi H, Higuchi H, Haseba Y and Iwata T 2007 *Soc. Inform. Disp. Symp. Digest* **38** 1737
- [22] Ge Z, Gauza S, Jiao M, Xianyu H and Wu S T 2009 *Appl. Phys. Lett.* **94** 101104
- [23] Bigelow J E and Kashnow R A 1977 *Appl. Opt.* **16** 2090
- [24] Zhu X, Ge Z and Wu S T 2006 *J. Disp. Technol.* **2** 2